

TI Designs: TIDA-01598

Reference Design for Low-Side, High-Bandwidth Current Amp and Error Detection for Solar Inverters



Description

This reference design provides a solution for an accurate shunt-based current measurement on the low side with an integrated fault-detection feature. It consists of a current sense amplifier which supports current sensing for a high bandwidth. The fault detection feature allows detection of undercurrent and overcurrent faults. The design provides a performance comparison between shunt-based current sensing and current sensing using a Hall sensor.

Resources

| | |
|-----------------------------|----------------|
| TIDA-01598 | Design Folder |
| INA240 | Product Folder |
| LMV393-N | Product Folder |
| TLV431 | Product Folder |
| OPA350 | Product Folder |
| SN74LVC1G17 | Product Folder |
| TPS717 | Product Folder |
| LP2985 | Product Folder |
| TLV760 | Product Folder |

Features

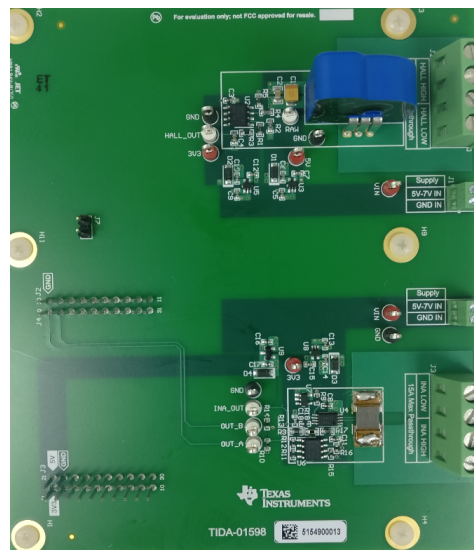
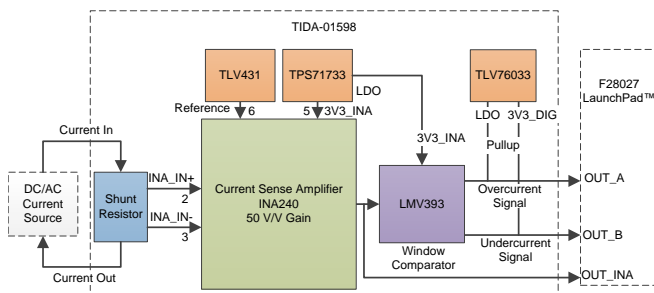
- Shunt-based low-side current sensing system with negative common-mode support
- Compact system for current sensing
- High bandwidth current sensing of up to 400kHz
- Bidirectional current-sensing support
- Integrated undercurrent and overcurrent detection with less than 1- μ s response time
- Less than 0.3% error in measurement for complete dc current range (-3 A to 15 A)
- Built-in 0.62 V_{REF} to level-shift output

Applications

- [Solar String Inverters](#)
- [Solar Central Inverters](#)



[ASK Our E2E™ Experts](#)





An IMPORTANT NOTICE at the end of this TI reference design addresses authorized use, intellectual property matters and other important disclaimers and information.

1 System Description

Solar panels consist of photovoltaic solar cells which harvest solar energy from the sun and generate electricity. The DC current and voltages generated in solar panels is then converted to AC to be fed in the grid. A string inverter is connected to multiple solar panels in series for this purpose. The current range generated by the panel typically varies from 12 A to 15 A. It is necessary to monitor this current to effectively operate the DC/DC MPPT input of the solar inverter. Additionally, in case of an overcurrent fault, the current exceeds the maximum current limit and thus can damage the power devices in the inverter. Reverse current faults where the current flows into the panels can damage the solar panels. Overcurrent and reverse current faults must be detected and resolved quickly.

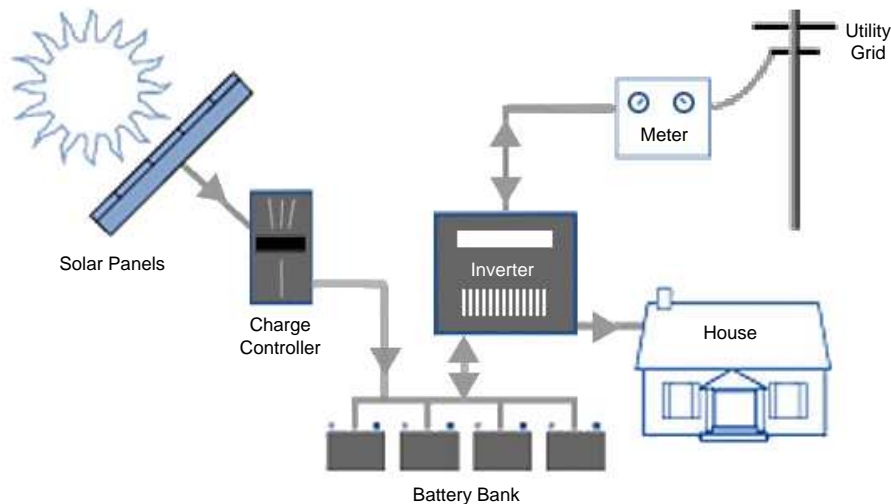


Figure 1. Typical Solar System

1.1 Current Monitoring

Current monitoring methods include high-side sensing and low-side sensing. In high-side sensing, the current-sensing element is connected between the supply and the load whereas in low-side sensing, the current sensing element is connected between the load and ground.

1.1.1 Hall Sensors

Closed-loop current transducers use a ferro-magnetic core with a sensing element or field probe inserted into a gap in the core. The core picks up the magnetic field created by the current flowing through the primary winding. Changes in the magnetic field are measured by the sense element and are passed on to a signal conditioning stage for filtering and amplification. The coil driver stage provides current to the compensation coil which creates an opposing magnetic field that cancels the effect of the primary current. The compensation current passes through a shunt resistor which provides a differential voltage to a precision sense amplifier. The amplifier gains the shunt voltage and drives the output stage of the transducer. The resulting voltage output is proportional to the current flowing through the primary winding as shown in the transfer function defined in [Equation 1](#). Additional amplification and scaling can be done before the signal reaches a system ADC.

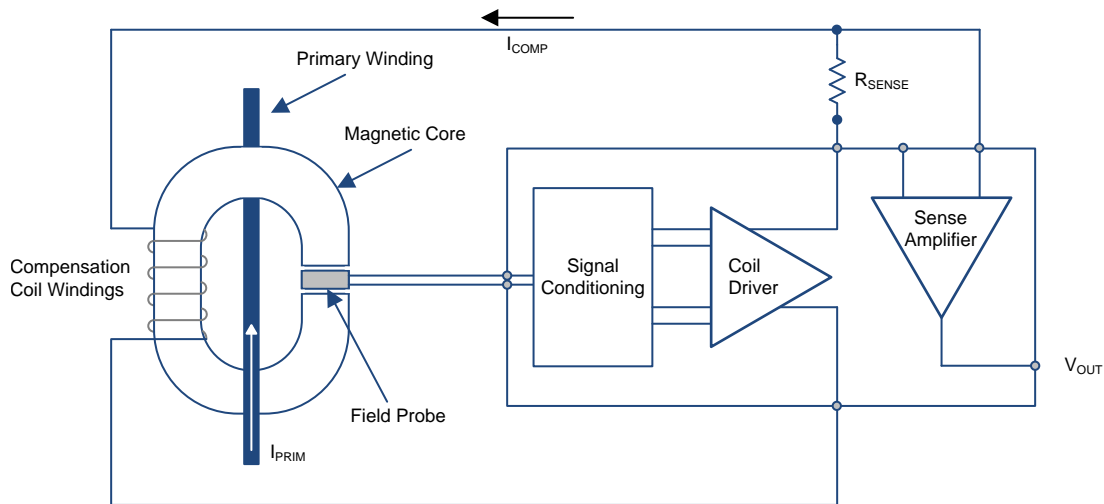


Figure 2. Closed-Loop Sensor Block Diagram

$$V_{OUT} = I_{PRIM} \times \left(\frac{N_p}{N_s} \right) \times R_{SENSE} \times \text{Gain} \quad (1)$$

By nature of the separation of the primary current carrier and the magnetic flux concentration coils, the Hall-effect sensor is inherently isolated. The physical limits of the sensor limit the overall total bandwidth to typically < 200 kHz. Additionally, the added complexity also increases cost versus other sensor solutions. For the TIDA-01598, an LEM LTS 15-NP Hall-effect sensor was placed beside the shunt-based solution to provide a direct comparison.

1.1.2 Shunt Sensors

Current sensing can be done by measuring the voltage drop across a shunt resistor. On the high side, current can be monitored directly from the source with immunity to ground disturbances. The common-mode range of the amplifier has to include the supply voltage which may exceed the supply voltage range, thus requiring isolation. Alternatively, low-side sensing can be used for which the common-mode voltage is zero.

Compared to magnetic-based sensing solutions, shunt sensors are very simple transducers capable of measuring a wide bandwidth current signal. However, they do lack the inherent galvanic isolation that comes with using a Hall sensor. Shunt sensors could also introduce undesired power loss in the system due to the voltage drop across the sensor. This power loss is dissipated as heat in the system, which could also influence nearby components negatively. Care must be taken to ensure that the power loss is minimized.

1.2 Low-Side Current Sensing

The low-side current-sensing module consists of the following subsystems:

1.2.1 Current Sensor

To read current, measure the voltage drop across a shunt resistor. Shunt resistors have a very low resistance value and cause a voltage drop of around 10 mV to 100 mV.

1.2.2 Signal Conditioning

A signal conditioning circuit is used to scale the low-voltage drop across the shunt element. The amplifier used for this purpose can be a precision op amp, instrumentation amplifier, programmable-gain amplifier, and a differential amplifier or isolation amplifier. The amplifier selection depends on the accuracy and temperature drift requirements. The TIDA-01598 uses a current sense amplifier with a fixed gain, high bandwidth, and also supports negative common-mode voltages.

1.2.3 Power Supply

The current-sensing module requires only an independent onboard supply ranging from 5 V to 6.5 V. Low dropout (LDO) regulators are used to provide a voltage supply to the current sense amplifier, comparator, Hall sensor, and scaling amplifier in the circuit.

Table 1. TIDA-01598 LDOs

| LDO REGULATOR | OUTPUT VOLTAGE | COMMENTS |
|---------------|-----------------|---|
| TPS717 | 3.3 V | Scaling amplifier, window comparator supply voltage |
| TLV760 | 3.3 V (Digital) | Pullup voltage |
| LP2985 | 5 V | Hall-sensor supply voltage |

1.2.4 Fault Current Detection

A fault detection circuit is used to detect overcurrent and negative current conditions. An arc can create faulty negative currents which must be detected. Dual comparators configured as window comparator circuit with low propagation delay can be used to generate voltage signals in case of a fault. The typical timing requirement of overcurrent and negative current fault detection is less than 2 μ s. This design achieves a system fault-detection response time of less than 1 μ s.

1.3 Featured Applications

The section provides information on different end equipment where low-side, high-bandwidth current amplification and fault detection can be used

1.3.1 Solar Inverters

Solar inverters are necessary for converting the DC voltage and currents generated by the solar panels to AC voltage and currents to feed in the grid. It is necessary to monitor current for efficiency and to protect sensitive devices. A shunt-based current-sensing device can be placed on the low side of each solar string and one at the common to effectively measure the current through each string of the solar string inverter. The output of the shunt sensor can then be used as the control algorithm input by a processing unit.

In an inverter with (N) solar string inputs, a TI design consisting of (N + 1) shunt-based sensors has a lower cost than (N) Hall sensors placed on the high side and shows better performance in terms of accuracy in current measurement, high-bandwidth sensing, and solution size. The TI design solution finds a similar application in solar central inverters.

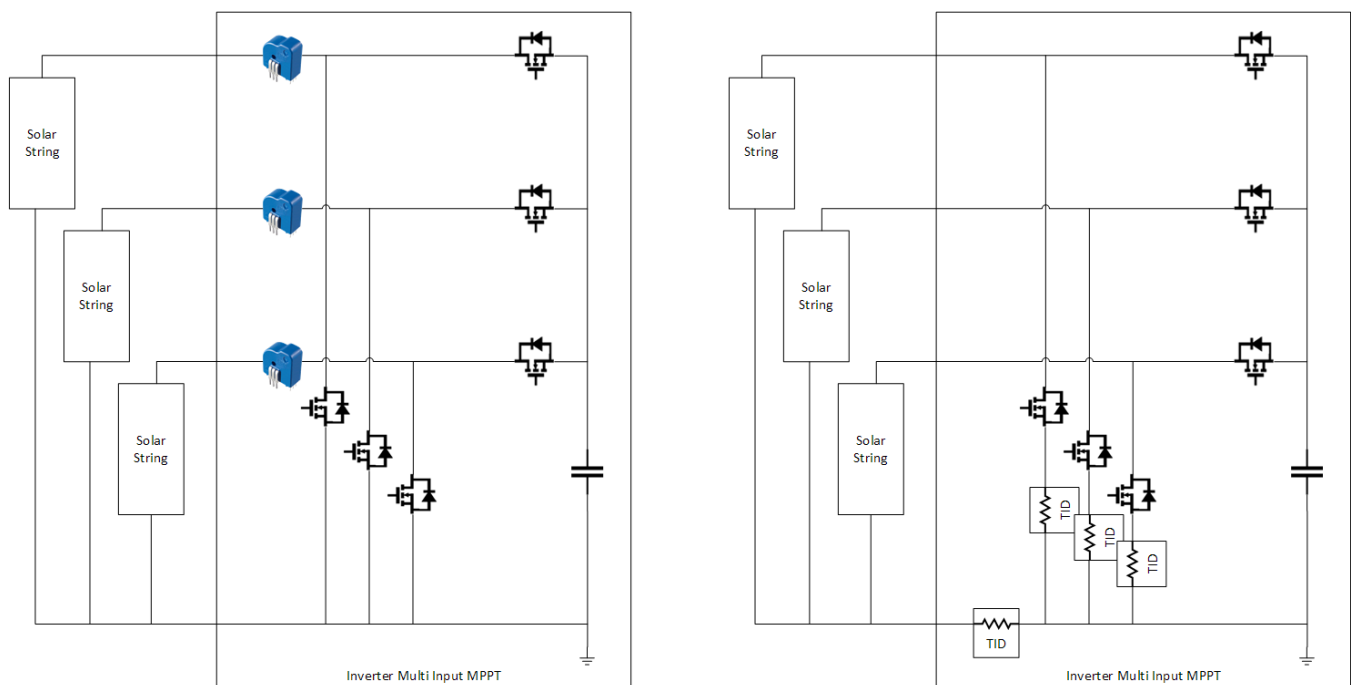


Figure 3. Current-Sensing Solution for a Solar Inverter Application Using a) Hall Sensors on High Side and b) Shunt-Based Low-Side Sensing

1.4 TI Design TIDA-01598 Advantages

This TI Design using a current sense amplifier with a fault detection circuit provides the following advantages over the design using Hall effect based sensors:

- Higher bandwidth sensing of up to 400 kHz is possible
- Smaller solution footprint
- Provides for an integrated overcurrent and undercurrent detection
- Provides a lower noise floor
- Reduced total solution cost

1.5 Key System Specifications

Table 2 shows key specifications provided by shunt-based current measurement.

Table 2. Key System Specifications

| PARAMETER | DESCRIPTION | COMMENTS |
|---------------------------|--|---|
| Current measurement range | Up to 15-A DC current | Up to 3-A negative current can be measured in case of a reverse current fault |
| Measurement accuracy | Less than 0.05% for the complete current range. | |
| AFE bandwidth | High-bandwidth sensing of up to 400 kHz | |
| Current shunt | Shunt resistor with low resistance and low temperature coefficient value | Equivalent shunt resistance formed by connecting two resistors in parallel to increase current carrying capacity and reduce potential critical faults if a shunt fails. |
| Amplifier | 50 V/V fixed gain, current sense amplifier | With adjustable reference voltage to vary current range in the positive or negative direction |
| Power supply | Onboard supply and LDO regulators | Low noise (30 μ V _{RMS}) |
| Window comparator | Dual comparator with a low propagation and resistive network to detect fault | According to overcurrent and undercurrent specifications |
| Dual comparator bandwidth | High-bandwidth support of up to 500 kHz | |
| Reference | Voltage shunt regulator to provide constant reference voltage to the current sense amplifier | According to the current-sensing range requirement in either direction |

2 System Overview

2.1 Block Diagram

This TI design TIDA-01598 showcases the following configuration for system performance comparison between:

- Current sense amplifier INA240 with fault detection
- Hall effect based current transducer with signal conditioning

2.1.1 Current-Sense Amplifier INA240 With Fault Detection

The current-sense amplifier INA240, with fault detection, has the following functional blocks:

- Current sense amplifier INA240 with 50 V/V gain to measure the voltage drop across the shunt resistor.
- Voltage shunt regulator to provide constant reference voltage to the INA240.
- LDO regulators to generate the required power supply.
- High-speed window comparator to detect overcurrent and undercurrent fault.

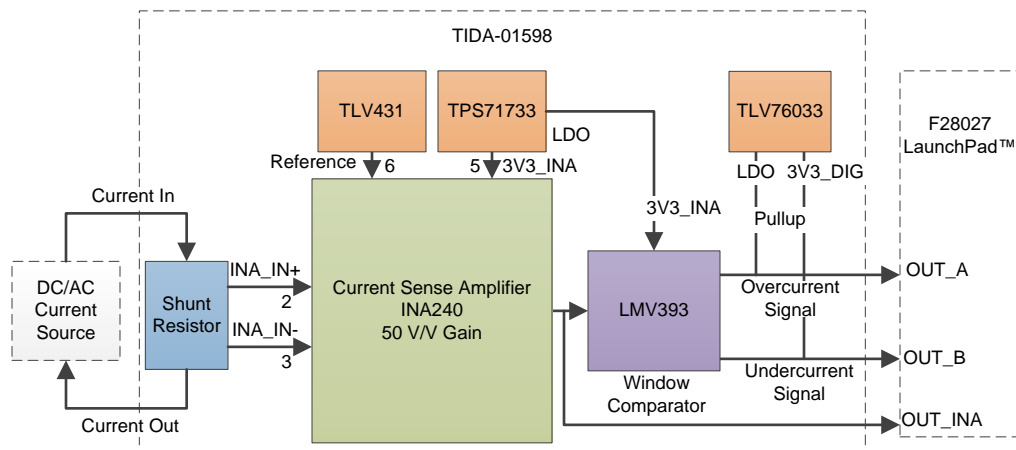


Figure 4. TIDA-01598 Shunt Block Diagram

2.1.2 Hall Effect Based Current Transducer With Signal Conditioning

The Hall effect based current transducer with signal conditioning has the following functional blocks:

- Hall effect based current transducer to sense current up to 15 A
- Low noise, LDOs to generate the required analog and digital power supply.
- Scaling op amp to scale the output of a Hall sensor according to the ADC input range.

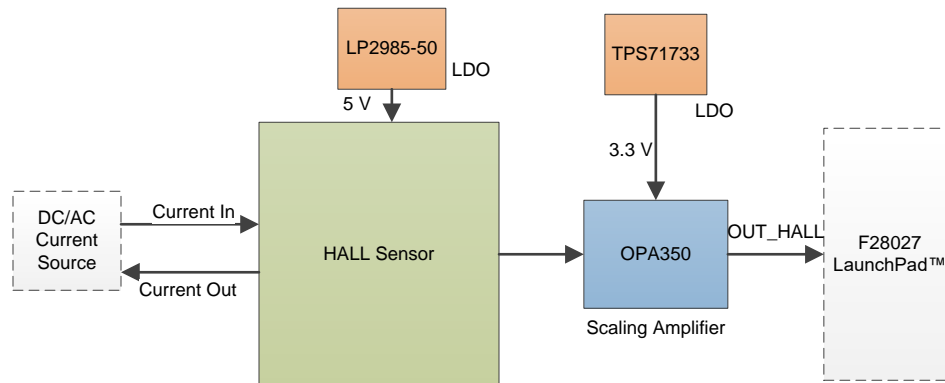


Figure 5. TIDA-01598 Hall Sensor Block Diagram

2.2 Highlighted Products

This section provides details on the TI products used in this TI design.

2.2.1 Bidirectional Current Sense Amplifier

2.2.1.1 INA240

The INA240 device is a bidirectional current sense amplifier with a wide common-mode range, zero drift topology, enhanced PWM rejection, and excellent CMRR. The device family offers four fixed gain values: 20 V/V, 50 V/V, 100 V/V and 500 V/V, and a high-gain accuracy with gain error less than 0.2% and low offset value allowing sensing of minimum a voltage drop as low as 10 mV. The reference voltage input of the device allows for both a positive and negative current range, according to requirement. For more information, see the [INA240 product page](#).

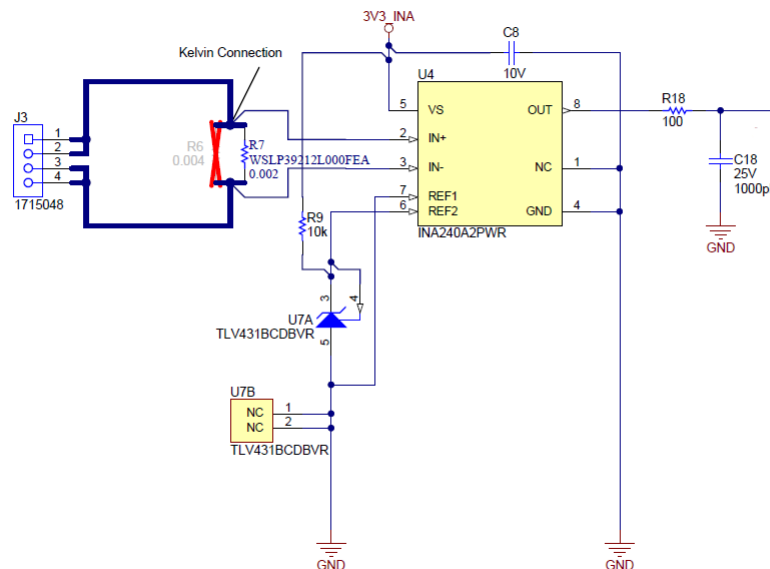


Figure 6. INA240 Connections

2.2.2 Design Enhancements

The following section provides some of the design enhancement options:

2.2.2.1 Shunt Resistor Selection and Sizing

The shunt resistor selection depends on the available supply voltage, full-scale current to be measured, and the current sense amplifier device gain. A minimum resistor can be chosen to maximize the current input range of the circuitry.

Shunt resistor size affects the current measurement accuracy and power dissipation across the resistor. A larger resistor improves the current measurement accuracy of the circuitry but also leads to increased power dissipation across the resistor. The heat generated due to the power dissipation may adversely affect the current measurement accuracy of the resistor due to the resistor temperature coefficient. Thus, this TI Design (TIDA-01598) uses a current shunt resistor with a temperature coefficient as low as ± 75 ppm/ $^{\circ}\text{C}$. Current sense amplifiers with higher gain are required if smaller shunt resistors are used which lead to increased error and noise parameters. This TI Design uses the INA240 device which maintains a high-performance level for higher gain settings.

Table 3 shows the steps for selection of shunt resistors for INA240 with 3.3-V supply voltage and current-sensing range of up to 15 A.

Table 3. INA240 Shunt Resistors

| PARAMETER | EQUATION | RESULTS |
|------------------------|--|---|
| INA240 output range | $V_{\text{GND}} + 1 \text{ mV} < V_{\text{OUT}} < V_{\text{S}} - 0.05 \text{ V}$ | $1 \text{ mV} < V_{\text{OUT}} < 3.25 \text{ V}$ |
| Gain | - | 50 V/V (INA240A2) |
| INA240 input range | $V_{\text{IN}} = (V_{\text{OUT}}) / 50$ | $20 \mu\text{V} < V_{\text{OUT}} < 0.065 \text{ V}$ |
| Current range | - | $0.25 \text{ A} < I_{\text{LOAD}} < 15 \text{ A}$ |
| $R_{\text{SHUNT-MAX}}$ | $V_{\text{IN-MAX}} / I_{\text{LOAD-MAX}}$ | 4.3 m Ω |
| $R_{\text{SHUNT-MIN}}$ | $V_{\text{IN-MIN}} / I_{\text{LOAD-MIN}}$ | 80 $\mu\Omega$ |

As resistor power dissipation leads in self heating and system power losses, choose the largest R_{SHUNT} that the system can tolerate.

2.2.2.2 Bidirectional Input Current Range

The INA240 reference can be configured to alter the bidirectional current ranges to be sensed. The device reference pins can be connected together to the positive rail for maximizing negative input current to be measured and to the negative rail for maximizing positive input current to be measured. The reference pins can be connected to an external reference for an output of reference voltage for shorted inputs. The output voltage will increase over the reference voltage for positive current and decrease under the reference voltage for negative current. Connecting one reference pin to positive rail and the other to the negative rail will allow equal current in either direction. The current configuration with one pin connected to reference voltage of 1.24 V and another pin to ground allows for positive current measurement of up to 15 A.

2.2.2.3 Comparator With Low Propagation Delay

Choose a window comparator with low propagation delay for fault detection at high frequencies. The LMV393 device can detect fault accurately for frequencies up to 500 kHz. The TLV3202 and TLV3502 devices are dual high-speed comparators with low propagation delay which can be used for higher frequency fault detection requirement. Table 4 compares the propagation delay for these three parts.

Table 4. Propagation Delay Comparison

| COMPARATOR PART NUMBER | DESCRIPTION | PROPAGATION DELAY |
|------------------------|--|-------------------|
| TLV3202 | Dual, microPower, rail-to-rail input comparator with push-pull outputs | 47 ns |

Table 4. Propagation Delay Comparison (continued)

| COMPARATOR PART NUMBER | DESCRIPTION | PROPAGATION DELAY |
|------------------------|--|-------------------|
| TLV3502 | Dual, rail-to-rail input comparator with push-pull outputs | 4.5 ns |
| LMV393 | Dual general purpose low-voltage comparator | 0.2 μ s |

3 Hardware, Software, Testing Requirements, and Test Results

3.1 Getting Started Hardware

This section describes the setup for testing the TIDA-01598.

3.1.1 Hardware

This section provides information on the different interface connectors for connecting the power supply and current input. Table 5 provides details on the different connectors used for applying the inputs and power supply for performance evaluation of the current sensing.

Table 5. Connector Functions

| CONNECTOR | FUNCTION | COMMENTS |
|------------|----------------------------------|---|
| J4 | DC power supply to INA240 | 5-V to 7-V DC Supply |
| J1 | DC power supply to Hall sensor | 5-V to 7-V DC Supply |
| J3.1, J3.2 | Input current IN to INA240 | |
| J3.3, J3.4 | Input current OUT to INA240 | |
| J2.3, J2.4 | Input current IN to Hall sensor | Current should not exceed 4.4 A _{RMS} and 25-A DC. |
| J2.1, J2.2 | Input current OUT to Hall sensor | |

3.1.2 Test Setup for Current Sensing

Figure 8 provides information on the setup used for current performance testing of the INA240-based current sense amplifier. The test setup for testing the TIDA-01598 consists of (1) DC power supply (–6 V), (2) TIDA-01598 TI design board, (3) AC current source, (4) DC source (10 V), (5) DC electronic load (programmable), (6) multimeter for measuring expected output voltage of the sensor.

NOTE: While testing, make sure the inputs do not exceed the range specified in Table 5 for proper operation.

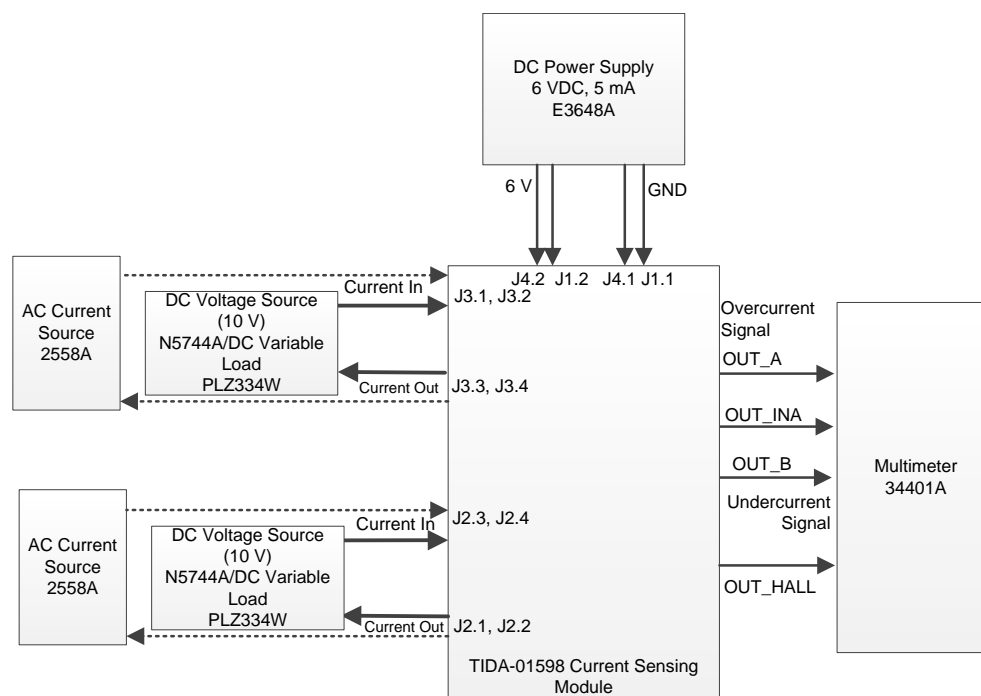


Figure 8. Setup for Testing Current Measurement Performance

3.2 Testing and Results

3.2.1 Simulation Results Using TINA-TI Software

The entire signal chain, including the INA240, LM393, TMS320C2x ADC input, and passive filters are simulated for AC transfer analysis and comparator response time using TINA-TI.

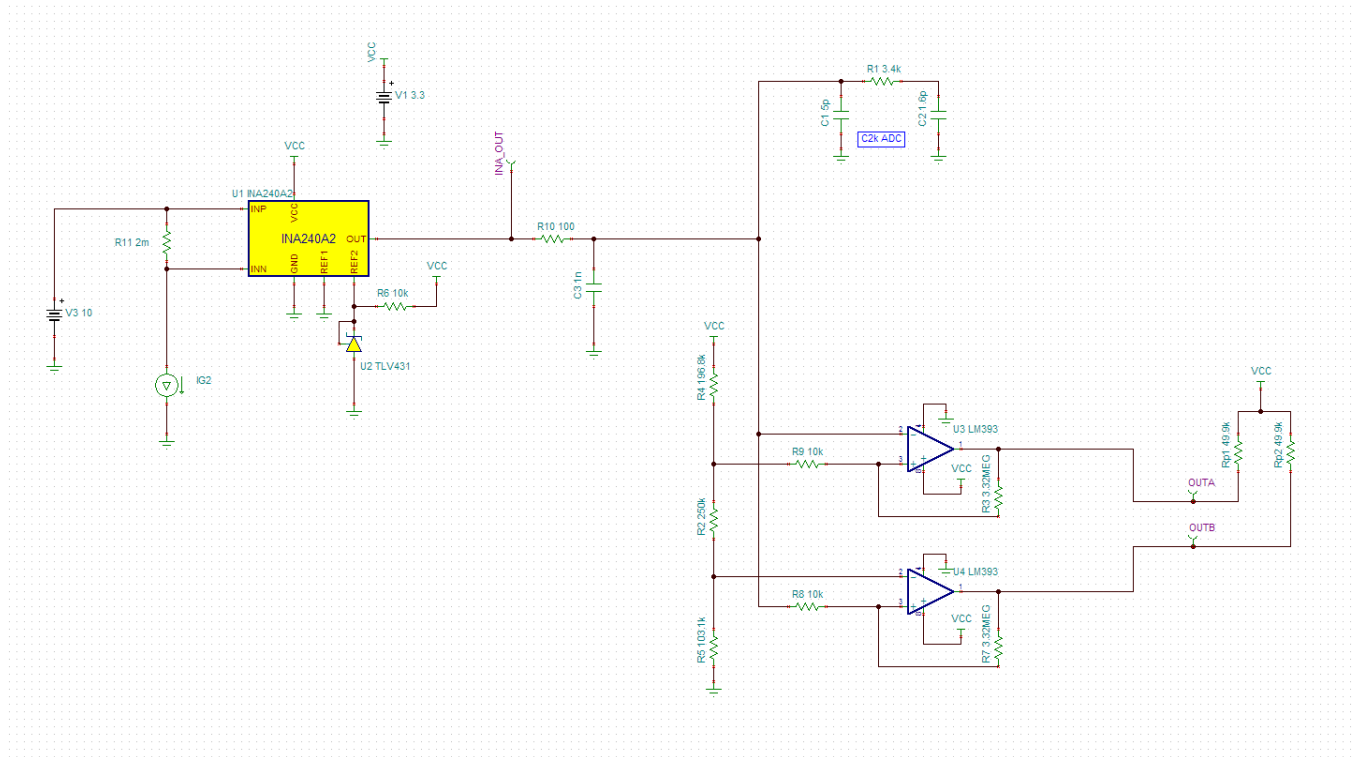


Figure 9. TIDA-01598 Simulation Model

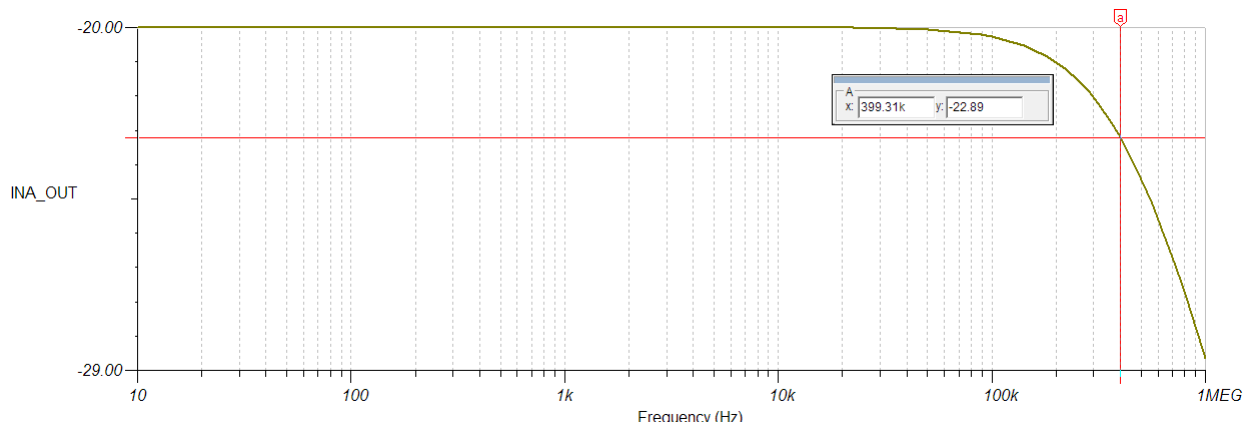


Figure 10. TIDA-01598 Frequency Response Simulation

Observe in [Figure 11](#) that the expected transfer of the analog current signal is still above the -3 -db drop point at the target frequency of 400 kHz.

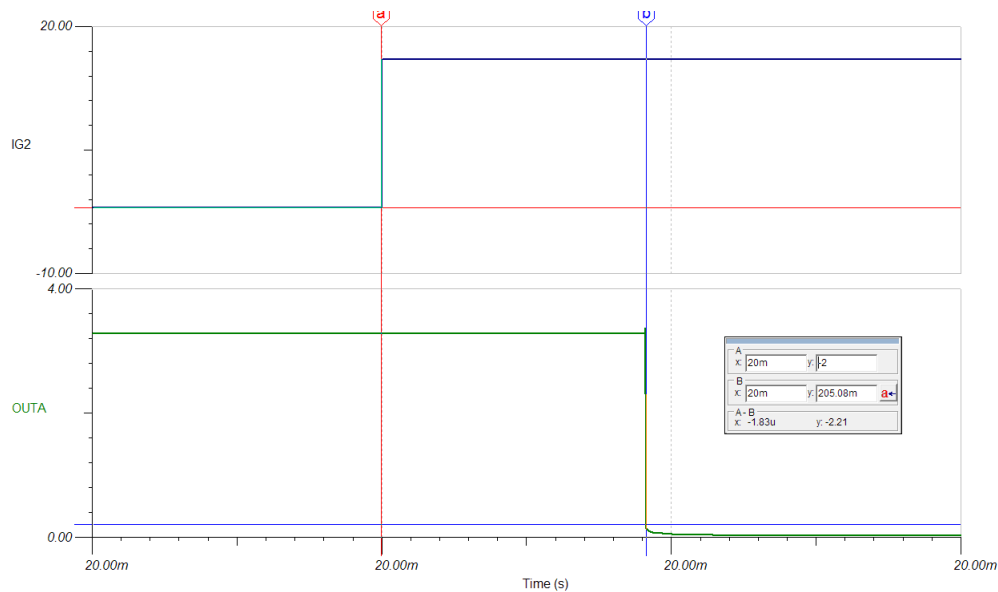


Figure 11. TIDA-01598 Overcurrent Response Simulation

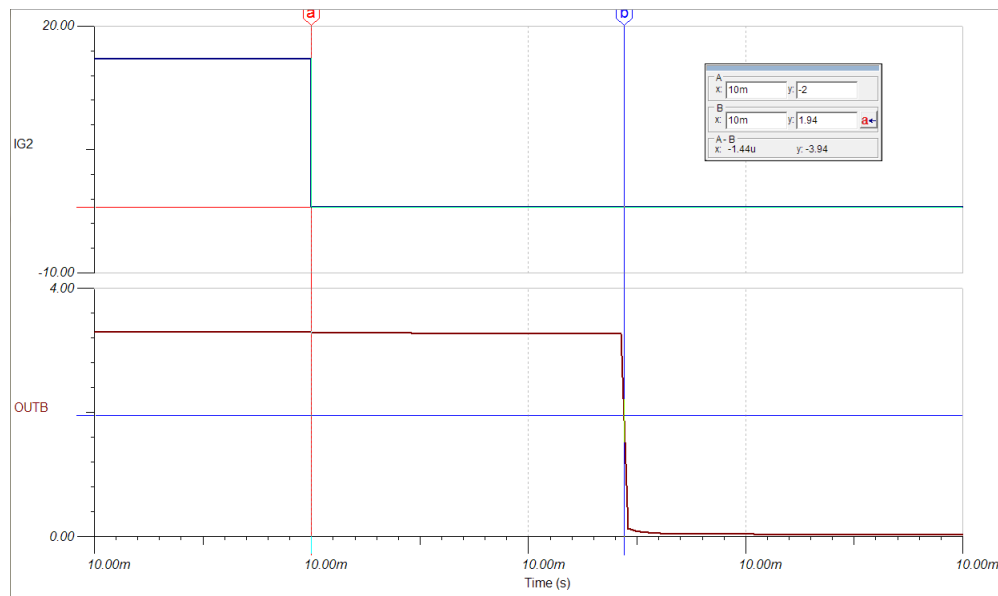


Figure 12. TIDA-01598 Undercurrent Response Simulation

To simulate an overcurrent and undercurrent event, a square current wave was pulsed through the shunt resistor that would force the event. The measured delay to the active-low system output was below the target of $2 \mu\text{s}$.

3.2.2 Functional Testing

The following test conditions are provided for performance measurement.

The tests were done using a function generator or programmable current source or programmable DC voltage source and load. A multimeter was used to record output values.

Table 6 provides details on the different functional tests that are done on the AIM.

Table 6. Functional Tests on the AIM

| PARAMETER | SPECIFICATION | MEASUREMENT |
|--|--------------------------------------|---------------|
| Observations for shunt-based current sensing: | | |
| 3.3-V LDO output | 3.3 V | 3.3 V |
| 3.3-V DIG LDO output | 3.3 V | 3.28 V |
| INA240 current sense amplifier | Measurement of current functionality | OK |
| Window comparator | Detection of fault up to 400 kHz | OK |
| Shunt regulator for external Reference output | 1.24 V | 1.2433 V |
| Observations for Hall effect-based current sensing: | | |
| 5-V LDO output | 5 V | 4.98 V |
| 3.3-V LDO output | 3.3 V | 3.3 V |
| HALL sensor-based current transducer | Measurement of current functionality | OK |
| Scaling amplifier | 1.66 V/V Gain | 1.66 V/V Gain |

3.2.3 DC Current Measurement Performance Testing

This section provides details of the DC current measurement performance testing observations for DC current input varying from 0.25 A to 15 A. The output measured was averaged over 250 readings on a 34401A multimeter.

The current shunt resistor value is 3 mΩ.

Table 7. Observation for Shunt-Based Current Sensing

| CURRENT INPUT | INA240 EXPECTED OUTPUT | INA240 MEASURED OUTPUT | OUTPUT ERROR (%) |
|---------------|------------------------|------------------------|------------------|
| 0.25 A | 0.6575 V | 0.6592 V | 0.26% |
| 0.5 A | 0.6950 V | 0.6969 V | 0.27% |
| 1 A | 0.7700 V | 0.7720 V | 0.26% |
| 1.5 A | 0.8450 V | 0.8475 V | 0.29% |
| 2 A | 0.9200 V | 0.9224 V | 0.26% |
| 3 A | 1.0700 V | 1.0730 V | 0.28% |
| 4 A | 1.2200 V | 1.2232 V | 0.26% |
| 5 A | 1.3700 V | 1.3737 V | 0.27% |
| 6 A | 1.5200 V | 1.5242 V | 0.27% |
| 7 A | 1.6700 V | 1.6741 V | 0.25% |
| 8 A | 1.8200 V | 1.8244 V | 0.24% |
| 9 A | 1.9700 V | 1.9751 V | 0.26% |
| 10 A | 2.1200 V | 2.1254 V | 0.25% |
| 12 A | 2.4200 V | 2.4260 V | 0.25% |
| 13 A | 2.5700 V | 2.5766 V | 0.26% |
| 14 A | 2.7200 V | 2.7271 V | 0.26% |
| 15 A | 2.8700 V | 2.8778 V | 0.27% |

The maximum error in the sensor output is 0.29% and the minimum error is 0.24%.

The variation of error in sensor output is 0.05% for the current range of 0.25 A to 15 A.

Table 8. Observation for Hall Effect-Based Current Sensing

| CURRENT INPUT | HALL EFFECT SENSOR EXPECTED OUTPUT | HALL EFFECT SENSOR MEASURED OUTPUT | OUTPUT ERROR (%) |
|---------------|------------------------------------|------------------------------------|------------------|
| 0.25 A | 2.5100 V | 2.5124 V | 0.08% |
| 0.5 A | 2.5210 V | 2.5230 V | 0.09% |
| 1 A | 2.5420 V | 2.5440 V | 0.09% |
| 1.5 A | 2.5630 V | 2.5650 V | 0.10% |
| 2 A | 2.5830 V | 2.5860 V | 0.10% |
| 3 A | 2.6250 V | 2.6281 V | 0.12% |
| 4 A | 2.6670 V | 2.6700 V | 0.13% |
| 5 A | 2.7080 V | 2.7118 V | 0.13% |
| 6 A | 2.7500 V | 2.7539 V | 0.14% |
| 7 A | 2.7920 V | 2.7959 V | 0.15% |
| 8 A | 2.8330 V | 2.8380 V | 0.16% |
| 9 A | 2.8750 V | 2.8800 V | 0.17% |
| 10 A | 2.9170 V | 2.9219 V | 0.18% |
| 12 A | 3.0000 V | 3.0062 V | 0.21% |
| 13 A | 3.0420 V | 3.0481 V | 0.21% |
| 14 A | 3.0830 V | 3.0902 V | 0.22% |
| 15 A | 3.1250 V | 3.1322 V | 0.23% |

The maximum error in the Hall effect based sensor output is 0.23% and the minimum error is 0.08%. The variation of error in sensor output is 0.15% for (0.25 A–15 A) current range.

Shunt-based current sensing has lower error variation of 0.05% for DC current input whereas Hall effect based current sensing has a higher variation error variation of 0.15% for (0.25 A–15 A) current range. This TI design provides low cost and small size shunt-based current sensing with a lower error of 0.05% along with an integrated overcurrent and negative current fault detection feature.

3.2.4 AC Current Measurement Performance Testing

This section provides detailed observation of AC Current Measurement Performance testing for varying current inputs from 0.5 A RMS to 11 A RMS at 50 Hz, 60 Hz, and 400 Hz. The output voltage of the INA240 was set at 1.65 V at 0-V differential input by connecting one reference pin to ground and another to the supply voltage of the device (3.3 V) increasing the bidirectional current-sensing range of INA240 for testing purposes.

The current shunt resistor value is 2 mΩ.

Table 9 and Table 10 show the test data observed at 50 Hz.:

Table 9. Observation for Shunt-Based Current Sensing

| INPUT CURRENT AT 50 Hz | INA240 EXPECTED OUTPUT | INA240 MEASURED OUTPUT | OUTPUT ERROR (%) |
|------------------------|------------------------|------------------------|------------------|
| 0.5 A | 0.050 V | 0.048 V | 0.24% |
| 1 A | 0.100 V | 0.097 V | 0.19% |
| 1.5 A | 0.150 V | 0.145 V | 0.33% |
| 2 A | 0.200 V | 0.193 V | 0.28% |
| 2.5 A | 0.250 V | 0.242 V | 0.33% |
| 3 A | 0.300 V | 0.290 V | 0.26% |
| 4 A | 0.400 V | 0.387 V | 0.30% |
| 5 A | 0.500 V | 0.484 V | 0.29% |
| 6 A | 0.600 V | 0.580 V | 0.33% |
| 7 A | 0.700 V | 0.677 V | 0.26% |

Table 9. Observation for Shunt-Based Current Sensing (continued)

| INPUT CURRENT AT 50 Hz | INA240 EXPECTED OUTPUT | INA240 MEASURED OUTPUT | OUTPUT ERROR (%) |
|------------------------|------------------------|------------------------|------------------|
| 8 A | 0.800 V | 0.774 V | 0.26% |
| 9 A | 0.900 V | 0.871 V | 0.24% |
| 10 A | 1.000 V | 0.968 V | 0.24% |
| 11 A | 1.100 V | 1.064 V | 0.24% |

The maximum error in the sensor output is 0.33% and minimum error is 0.19%. The variation of error in sensor output is 0.14% for (0.5 A–11 A) current range.

Table 10. Observation for Hall Effect-Based Current Sensing

| INPUT CURRENT AT 50 Hz | HALL EFFECT SENSOR EXPECTED OUTPUT | HALL EFFECT SENSOR MEASURED OUTPUT | OUTPUT ERROR (%) |
|------------------------|------------------------------------|------------------------------------|------------------|
| 0.5 A | 0.0208 V | 0.0209 V | 0.53% |
| 1 A | 0.0417 V | 0.0419 V | 0.63% |
| 1.5 A | 0.0625 V | 0.0629 V | 0.64% |
| 2 A | 0.0833 V | 0.0839 V | 0.68% |
| 2.5 A | 0.1042 V | 0.1048 V | 0.60% |
| 3 A | 0.1250 V | 0.1257 V | 0.58% |
| 4 A | 0.1667 V | 0.1676 V | 0.54% |
| 5 A | 0.2083 V | 0.2095 V | 0.56% |
| 6 A | 0.2500 V | 0.2514 V | 0.54% |
| 7 A | 0.2917 V | 0.2934 V | 0.58% |
| 8 A | 0.3333 V | 0.3352 V | 0.55% |
| 9 A | 0.3750 V | 0.3771 V | 0.56% |
| 10 A | 0.4167 V | 0.4190 V | 0.55% |
| 11 A | 0.4583 V | 0.4609 V | 0.56% |

The maximum error in the sensor output is 0.68% and minimum error is 0.53%.

The variation of error in sensor output is 0.15% for (0.5 A–11 A) current range.

Shunt-based current sensing has lower error variation of 0.14% for AC current input range (0.5 A–11 A) at 50 Hz whereas Hall effect based current sensing has a higher error variation of 0.15%.

[Table 11](#) and [Table 12](#) show the test data observed at 60 Hz for 0.5 A to 11 A RMS input current range:

Table 11. Observation for Shunt-Based Current Sensing

| INPUT CURRENT AT 60 Hz | INA240 EXPECTED OUTPUT | INA240 MEASURED OUTPUT | OUTPUT ERROR (%) |
|------------------------|------------------------|------------------------|------------------|
| 0.5 A | 0.050 V | 0.048 V | 0.21% |
| 1 A | 0.100 V | 0.097 V | 0.24% |
| 2 A | 0.200 V | 0.193 V | 0.28% |
| 6 A | 0.600 V | 0.580 V | 0.27% |
| 11 A | 1.100 V | 1.065 V | 0.22% |

The calibration factor at output is 3.

The maximum error in the sensor output is 0.28% and the minimum error is 0.21%. The variation of error in the sensor output is 0.07% for (0.5 A–11 A) current range.

Table 12. Observation for Hall Effect-Based Current Sensing

| INPUT CURRENT AT 60 Hz | HALL EFFECT SENSOR EXPECTED OUTPUT | HALL EFFECT SENSOR MEASURED OUTPUT | OUTPUT ERROR (%) |
|------------------------|------------------------------------|------------------------------------|------------------|
| 0.5 A | 0.021 V | 0.021 V | 0.62% |
| 1 A | 0.042 V | 0.042 V | 0.51% |
| 2 A | 0.083 V | 0.084 V | 0.52% |
| 6 A | 0.250 V | 0.251 V | 0.42% |
| 11 A | 0.458 V | 0.460 V | 0.44% |

The maximum error in the sensor output is 0.62% and the minimum error is 0.44%. The variation of error in the sensor output is 0.18% for (0.5 A–11 A) current range.

Shunt-based current sensing has a lower error variation of 0.07% for AC current input range (0.5 A–11 A) at 60 Hz; whereas Hall effect-based current sensing has a higher error variation of 0.18%.

Table 13 and Table 14 show the test data observed at 400 Hz for 0.5 A to 11 A RMS input current range:

Table 13. Observation for Shunt-Based Current Sensing

| INPUT CURRENT AT 400 Hz | INA240 EXPECTED OUTPUT | INA240 MEASURED OUTPUT | OUTPUT ERROR (%) |
|-------------------------|------------------------|------------------------|------------------|
| 0.5 A | 0.050 V | 0.048 V | 0.16% |
| 1 A | 0.100 V | 0.097 V | 0.20% |
| 2 A | 0.200 V | 0.193 V | 0.26% |
| 6 A | 0.600 V | 0.581 V | 0.25% |
| 11 A | 1.100 V | 1.065 V | 0.20% |

The maximum error in the sensor output is 0.26% and the minimum error is –0.16%. The variation of error in the sensor output is 0.10% for the (0.5 A–11 A) current range

Table 14. Observation for Hall Effect-Based Current Sensing

| INPUT CURRENT AT 400 Hz | HALL EFFECT SENSOR EXPECTED OUTPUT | HALL EFFECT SENSOR MEASURED OUTPUT | OUTPUT ERROR (%) |
|-------------------------|------------------------------------|------------------------------------|------------------|
| 0.5 A | 0.021 V | 0.021 | 0.848% |
| 1 A | 0.042 V | 0.042 | 0.754% |
| 2 A | 0.083 V | 0.084 | 0.748% |
| 6 A | 0.250 V | 0.252 | 0.619% |
| 11 A | 0.458 V | 0.461 | 0.617% |

The maximum error in the sensor output is 0.848% and the minimum error is 0.617%. The variation of error in the sensor output is 0.23% for (0.5 A–11 A) current range.

Shunt-based current sensing has a lower error variation of 0.10% for AC current input range (0.5 A–11 A) at 400 Hz; whereas the Hall effect-based current sensing has a higher error variation of 0.23%.

3.2.4.1 Summary of AC Current Measurement Performance Testing

Table 15. AC Current Measurement Performance Testing

| FREQUENCY | INPUT CURRENT RANGE | VARIATION IN ERROR FOR SHUNT-BASED SENSING (%) | VARIATION IN ERROR FOR HALL EFFECT BASED SENSING |
|-----------|---------------------|--|--|
| 50 Hz | 0.5 A–11 A | 0.14% | 0.15% |
| 60 Hz | 0.5 A–11 A | 0.07% | 0.18% |
| 400 Hz | 0.5 A–11 A | 0.10% | 0.23% |

Shunt-based current sensing has a lower error for AC current input range 0.5 A, 11 A at 50 Hz, 60 Hz and 400 Hz than Hall effect-based current sensing.

3.2.5 Fault Detection Performance Testing

3.2.5.1 Comparator Response Time

This section provides details of fault detection performance testing. A function generator was used to provide an input square wave to the comparator and the response time of the comparators was observed using an oscilloscope.

Table 16. Comparator Response Time

| COMPARATOR | PULLUP RESISTOR VALUE | DELAY IN OVERCURRENT DETECTION | DELAY IN UNDERCURRENT DETECTION |
|------------|-------------------------|--------------------------------|---------------------------------|
| LM393A | 3.3 k Ω | 1.24 μ s | 208 ns |
| LMV393 | 3.3 k Ω | 148 ns | 136 ns |
| TLC372 | 3.3 k Ω | 500 ns | 148 ns |
| TLV3202 | Internal pullup network | 48 ns | 56 ns |

The TIDA-01598 uses an LMV393 comparator for fault detection as it shows a low delay in overcurrent and undercurrent detection at lower cost. The delay for overcurrent detection is 148 ns and the delay for undercurrent detection is 136 ns.

The resistance value of the pullup resistors can be lowered to reduce the rise time delay shown by the comparator. [Table 17](#) shows the variation in delay of the LM393 comparator output with a change in the pullup resistor.

Table 17. LM393 Comparator Output Delay Variation

| COMPARATOR | PULLUP RESISTOR VALUE | DELAY IN RISE TIME |
|------------|-----------------------|--------------------|
| LM393A | 3.3 k Ω | 1.24 μ s |
| LM393A | 2.7 k Ω | 1.20 μ s |

3.2.5.2 System Fault Response Time

A function generator was used to provide an input square wave to the input of INA240 and the response time was observed using an oscilloscope. This will include any delay inherent in the INA240, providing a full system response time. The delay between a high input transition and the active-low state of OUT_A is the system overcurrent detection delay. Undercurrent response time is measured by the delay between a low input transition and the active-low output of OUT_B. These delays are illustrated in Figure 13 and Figure 14.

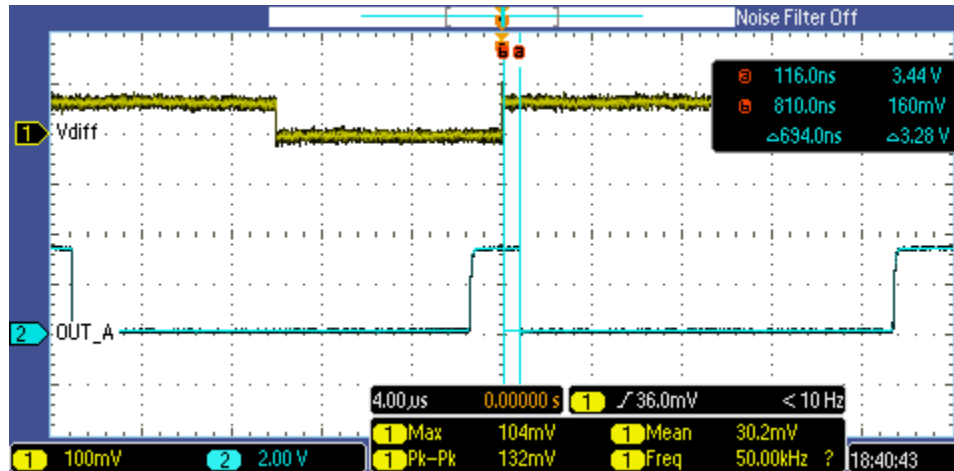


Figure 13. Overcurrent Detection Delay at 50 kHz

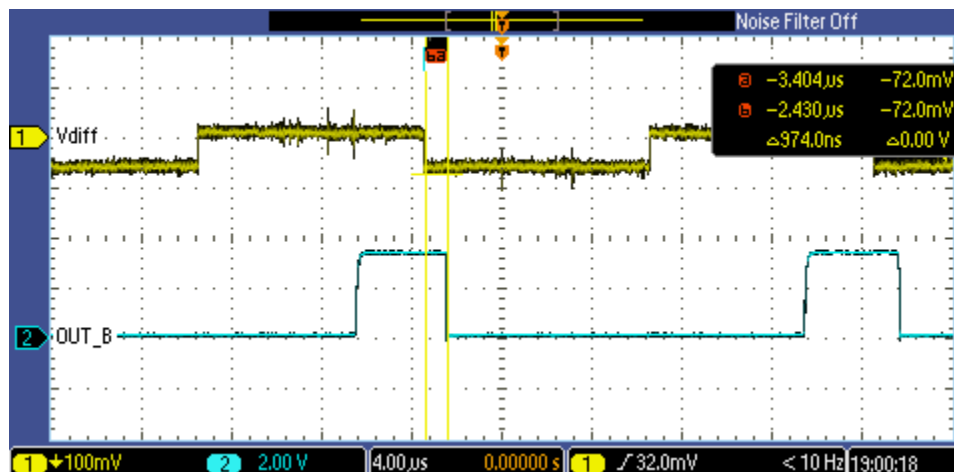


Figure 14. Undercurrent Detection Delay at 50 kHz

Table 18. Overcurrent and Undercurrent Fault System Delay

| COMPARATOR | PULLUP RESISTOR | INPUT FREQUENCY | OVERCURRENT DELAY | UNDERCURRENT DELAY |
|------------|-----------------|-----------------|-------------------|--------------------|
| LMV393 | 3.3 k Ω | 50 kHz | 900 ns | 990 ns |
| | | 100 kHz | 780 ns | 1 μ s |
| | | 400 kHz | 880 ns | 806 ns |
| | 2.7 k Ω | 50 kHz | 894 ns | 874 ns |
| | | 100 kHz | 708 ns | 714 ns |
| | | 400 kHz | 894 ns | 866 ns |

3.2.6 Test Results Summary

Table 19 summarizes the test and observations for the TIDA-01598 TI design.

Table 19. Test Results Summary

| TEST | OBSERVATION |
|------------------------------------|-------------|
| DC current measurement performance | OK |
| AC current measurement performance | OK |
| LDO output | OK |
| Reference voltage output | OK |
| Scaling amplifier | OK |
| Fault detection | OK |

4 Design Files

4.1 Schematics

To download the schematics, see the design files at [TIDA-01598](#).

4.2 Bill of Materials

To download the bill of materials (BOM), see the design files at [TIDA-01598](#).

4.3 PCB Layout Recommendations

4.3.1 Layout Prints

To download the layer plots, see the design files at [TIDA-01598](#).

4.4 Altium Project

To download the Altium Designer® project files, see the design files at [TIDA-01598](#).

4.5 Gerber Files

To download the Gerber files, see the design files at [TIDA-01598](#).

4.6 Assembly Drawings

To download the assembly drawings, see the design files at [TIDA-01598](#).

5 Related Documentation

1. Texas Instruments, [INA240 High- and Low-Side, Bidirectional, Zero-Drift, Current-Sense Amplifier With Enhanced PWM Rejection Data Sheet](#)
2. Texas Instruments, [LMV33x-N / LMV393-N General-Purpose, Low-Voltage, Tiny Pack Comparators Data Sheet](#)
3. Texas Instruments, [TLV431x Low-Voltage Adjustable Precision Shunt Regulator Data Sheet](#)
4. Texas Instruments, [OPAx350 High-Speed, Single-Supply, Rail-to-Rail Operational Amplifiers MicroAmplifier Series Data Sheet](#)
5. Texas Instruments, [SN74LVC1G17 Single Schmitt-Trigger Buffer Data Sheet](#)
6. Texas Instruments, [TPS717 Low-Noise, High-Bandwidth PSRR, Low-Dropout, 150-mA Linear Regulator Data Sheet](#)
7. Texas Instruments, [LP2985 150-mA Low-noise Low-dropout Regulator With Shutdown Data Sheet](#)
8. Texas Instruments, [TLV760 100-mA, 30-V, Fixed-Output, Linear-Voltage Regulator Data Sheet](#)

5.1 Trademarks

E2E is a trademark of Texas Instruments.

Altium Designer is a registered trademark of Altium LLC or its affiliated companies.

All other trademarks are the property of their respective owners.

6 About the Author

Vaibhavi Shanbhag is a project trainee in the Industrial Systems team at Texas Instruments where she is responsible for developing reference design solutions with a focus on Grid Infrastructure. Vaibhavi is a final-year student pursuing a Bachelor of Engineering (B.E. Hons.) in Electrical and Electronics Engineering from Birla Institute of Technology & Sciences (BITS), Pilani K.K.Birla Goa Campus.

BART BASILE is a systems architect in the Grid Infrastructure Solutions Team at Texas Instruments, where he focuses on renewable energy and EV infrastructure. Bart works across multiple product families and technologies to leverage the best solutions possible for system level application design. Bart received his bachelors of science in electronic engineering from Texas A&M University.

IMPORTANT NOTICE FOR TI DESIGN INFORMATION AND RESOURCES

Texas Instruments Incorporated ("TI") technical, application or other design advice, services or information, including, but not limited to, reference designs and materials relating to evaluation modules, (collectively, "TI Resources") are intended to assist designers who are developing applications that incorporate TI products; by downloading, accessing or using any particular TI Resource in any way, you (individually or, if you are acting on behalf of a company, your company) agree to use it solely for this purpose and subject to the terms of this Notice.

TI's provision of TI Resources does not expand or otherwise alter TI's applicable published warranties or warranty disclaimers for TI products, and no additional obligations or liabilities arise from TI providing such TI Resources. TI reserves the right to make corrections, enhancements, improvements and other changes to its TI Resources.

You understand and agree that you remain responsible for using your independent analysis, evaluation and judgment in designing your applications and that you have full and exclusive responsibility to assure the safety of your applications and compliance of your applications (and of all TI products used in or for your applications) with all applicable regulations, laws and other applicable requirements. You represent that, with respect to your applications, you have all the necessary expertise to create and implement safeguards that (1) anticipate dangerous consequences of failures, (2) monitor failures and their consequences, and (3) lessen the likelihood of failures that might cause harm and take appropriate actions. You agree that prior to using or distributing any applications that include TI products, you will thoroughly test such applications and the functionality of such TI products as used in such applications. TI has not conducted any testing other than that specifically described in the published documentation for a particular TI Resource.

You are authorized to use, copy and modify any individual TI Resource only in connection with the development of applications that include the TI product(s) identified in such TI Resource. NO OTHER LICENSE, EXPRESS OR IMPLIED, BY ESTOPPEL OR OTHERWISE TO ANY OTHER TI INTELLECTUAL PROPERTY RIGHT, AND NO LICENSE TO ANY TECHNOLOGY OR INTELLECTUAL PROPERTY RIGHT OF TI OR ANY THIRD PARTY IS GRANTED HEREIN, including but not limited to any patent right, copyright, mask work right, or other intellectual property right relating to any combination, machine, or process in which TI products or services are used. Information regarding or referencing third-party products or services does not constitute a license to use such products or services, or a warranty or endorsement thereof. Use of TI Resources may require a license from a third party under the patents or other intellectual property of the third party, or a license from TI under the patents or other intellectual property of TI.

TI RESOURCES ARE PROVIDED "AS IS" AND WITH ALL FAULTS. TI DISCLAIMS ALL OTHER WARRANTIES OR REPRESENTATIONS, EXPRESS OR IMPLIED, REGARDING TI RESOURCES OR USE THEREOF, INCLUDING BUT NOT LIMITED TO ACCURACY OR COMPLETENESS, TITLE, ANY EPIDEMIC FAILURE WARRANTY AND ANY IMPLIED WARRANTIES OF MERCHANTABILITY, FITNESS FOR A PARTICULAR PURPOSE, AND NON-INFRINGEMENT OF ANY THIRD PARTY INTELLECTUAL PROPERTY RIGHTS.

TI SHALL NOT BE LIABLE FOR AND SHALL NOT DEFEND OR INDEMNIFY YOU AGAINST ANY CLAIM, INCLUDING BUT NOT LIMITED TO ANY INFRINGEMENT CLAIM THAT RELATES TO OR IS BASED ON ANY COMBINATION OF PRODUCTS EVEN IF DESCRIBED IN TI RESOURCES OR OTHERWISE. IN NO EVENT SHALL TI BE LIABLE FOR ANY ACTUAL, DIRECT, SPECIAL, COLLATERAL, INDIRECT, PUNITIVE, INCIDENTAL, CONSEQUENTIAL OR EXEMPLARY DAMAGES IN CONNECTION WITH OR ARISING OUT OF TI RESOURCES OR USE THEREOF, AND REGARDLESS OF WHETHER TI HAS BEEN ADVISED OF THE POSSIBILITY OF SUCH DAMAGES.

You agree to fully indemnify TI and its representatives against any damages, costs, losses, and/or liabilities arising out of your non-compliance with the terms and provisions of this Notice.

This Notice applies to TI Resources. Additional terms apply to the use and purchase of certain types of materials, TI products and services. These include; without limitation, TI's standard terms for semiconductor products (<http://www.ti.com/sc/docs/stdterms.htm>), [evaluation modules](#), and [samples](http://www.ti.com/sc/docs/sampterm.htm) (<http://www.ti.com/sc/docs/sampterm.htm>).

Mailing Address: Texas Instruments, Post Office Box 655303, Dallas, Texas 75265
Copyright © 2018, Texas Instruments Incorporated